International Journal of Power and Energy Systems, Vol. 44, No. 10, 2024
An Open Access Paper

CHAIN FAULT IDENTIFICATION AND POWER GRID PLANNING OPTIMISATION IN POWER SYSTEMS CONSIDERING MULTIPLE SCENARIOS

Wenhua Guo*

Abstract

The study proposes a method for chained fault identification in power systems across various scenarios. It combines fault data and state search for fault identification, utilises a multi-scenario multi-objective optimisation method, and applies the fast non-dominated sorting genetic algorithm (NSGA-II) with elite strategy for optimal solution finding. This method enables a comprehensive analysis of chained fault identification and power grid planning in composite power systems. The simulation results demonstrated that 15,590 fault chains were obtained, updating the state fault network 29 times in a total time of 101.68 s. On average, each update took 0.197 s, while constructing the state fault network took 4,618.10 s. In comparison, the Monte Carlo sampling simulation completed 50,481 samples in 7,694.79 s, significantly less than the Monte Carlo simulation. The proposed method displays high computational efficiency and accuracy in identifying and analysing power system faults across multiple scenarios, which is crucial for security management.

Key Words

Power system, chain failure, multiple scenarios, power grid planning, fault identification

Nomenclature

l represents line. p_l represents the current transmission power of line l. $p_l^{\max}$ represents the transmission power limit of the line l. n represents the number of components included in a system. $f_{(k)}$ represents the number of faulty components. s_0 represents the initial state of the system, with $s_0 = 0^{1\times n}$. $N_{k,s}$ represents the state located in the k fault stage. $N_{k,f}$ represents number of faults located in the k stage. S represents the state value that can measure the risk of cascading failures of the system in that state. F represents the fault value that can be used to identify key components of the system and measure the risk of cascading failures in the system after the occurrence of the fault. $N_{s_{k(j)}}$ represents the number of occurrences of state $s_{k(j)}$ recorded in the fault data. f_l represents the actual faults of other components. z_i represents the power outage loss ultimately recorded in the i fault chain. $\breve{z}\left(s_k^i\right)$ represents the load loss generated at the state s_k^i. $\Pr\left(s_{k(j)}\right)$ represents the probability of convergence to the corresponding state occurs as the total amount of simulation sampling increases. $s_{k+1(j')}$ represents the states. $\Pr\left(s_{k+1(j')}\right)$ represents the probability of the subsequent state $s_{k+1(j')}$ when a fault is disconnected during the search process. $s_{k+1(j')}$ represents the subsequent status. $S^w\left(s_{k(j)}\right)$ represents the S value of the scenario w corresponding to the state $s_{k(j)}$. w represents the scene. $N^w_{s_{k(j)}}$ represents the record state $s_{k(j)}$ from the scenario w in the fault data. $N^w_{\left(s_{k(j)},f_m\right)}$ represents the number of occurrences of f_m from the scenario w in the state $s_{k(j)}$ in the fault data. $l = [l_1, l_2, \ldots, l_k]^T$ represents the expanded line vector. $u = [u_1, u_2, \ldots, u_k]^T$ represents the expansion capacity vector. $c = [c_1, c_2, \ldots, c_k]^T$ represents the expansion unit price vector. $G = \{w_1, \ldots, w_g\}$ represents the scenario after the expansion of the system, also known as the peak load mode scenario. $C_{\max}$ represents the upper limit of the total cost for the system expansion. α_k represents the maximum expansion capacity of the line l_k. p_l^c represents the rated transmission power of the line l. $\sigma\left(s_{k(j)}, f\right)$ represents the fault losses. $\left\{f_{(1)}, \ldots, f_{(k)}\right\}$ represents a fault chain of length k recorded. $F^w\left(s_{k(j)}, f_m\right)$ represents the F value of the scenario w corresponding to the state $s_{k(j)}$. $\left(s_0, f_{(1)}\right), \left(s_1, f_{(2)}\right), \ldots, \left(s_k, f_{(0)}\right)$ represent the pairing state with the corresponding faults in the fault

* Shanxi Railway Vocational and Technical College, Shaanxi, China
Corresponding author: Wenhua Guo

(DOI: 10.2316/J.2024.203-0536)

chain to form a sequence of binary tuples. N_c represents the total number of scenarios. $s_{k(j)}$ represents the k state located in the j fault stage. (u, l) represents a line expansion plan. $N_{\left(s_{k(j)}, f_l\right)}$ represents the number of occurrences of f_l in the state $s_{k(j)}$. $r^G(u, l)$ represents the multi-scenario cascading fault risk calculated based on the composite state fault network after applying the expansion plan. s_k represents the state of the k lines failure. N_M represents the total simulation sampling amount. $\Pr_0\left(s_{k(j)}, f_l\right)$ represents no probability of failure occurring.

1. Introduction

The power system is an indispensable infrastructure in modern society, whose function is to transmit electricity from power stations to users, providing the necessary power supply for people's daily lives and various industrial and commercial activities. To ensure the safe and reliable operation of the power system, fault identification, and processing technology in the power system has become one of the focuses of research [1]. The study focuses on the uninterrupted operation of the power system and addresses the impact of scenario and environmental changes. It analyses chain fault identification in the power system using fault data and state search [2]. The proposed method involves a multi-scenario approach to identify chain faults, combining multi-objective algorithms with genetic algorithms. Specifically, it utilises the fast and elitist non-dominated sorting genetic algorithm (NSGA-II) with elite strategies to find the Pareto-optimal solution set for fault identification and optimise the grid planning scheme. This approach is innovative in dealing with chain fault identification in multi-scenario power systems, which can improve the compatibility and stability of the power system and reduce the operational risks due to environmental changes or scenario switching. It provides new ideas for power system planning and operation and helps to improve the operational efficiency and stability of the power grid. The study is structured as follows: the first part outlines the purpose of the proposed power system chain fault identification. The second part provides background information and explains the significance of the research on the power system chain fault problem, including the methodology used. The third part focuses on the chain fault identification methodology based on fault data and state search and optimises the multi-scenario fault identification and power grid planning using NSGA-II. This section represents the innovation and focus of the research. The fourth part describes the experimental validation based on the algorithm designed in the second part, as well as the measurement and analysis of the experimental data results. The fifth part concludes the experimental results, highlights the limitations of the design, and discusses future research directions for further fault analysis.

2. Related Works

There are also some safety hazards in the operation of the power system, such as power failures. These faults have had a significant impact on the normal operation of the power system. Chain failures can cause major power outages in the power system, causing serious economic losses to society. In the study of multi-scenario and multi-objective power system optimisation, Li *et al.* proposed a long-term multi-region power system planning model that described the fluctuations of renewable electricity. Scenario analysis was used to address the policy uncertainty of carbon tax and electricity substitution. The results indicated that the model was effective for power system planning [3]. Martínez and Cruz-Mendoza analysed the power energy system to achieve gradual decarbonisation and integrate more intermittent renewable energy sources. They introduced a novel and flexible modeling method for power planning tools, which combined linear programming optimisation with computational strategies. This method enabled the efficient optimization of a wide range of economic and technical parameters in complex interconnected power systems, including reading, processing, and writing large amounts of data. The time consumption was optimised through binary matrices, and the results showed that it achieved energy recycling and efficiency [4]. Considering the prediction uncertainty of distributed generation and multi-energy loads, Mei *et al.* proposed a stochastic optimal operation model based on multi-scenario simulation. Based on Latin hypercube sampling for operation scenario generation, a stochastic optimal operation model with the overall operating economy as the decision-making objective was proposed based on typical operation scenarios. The effectiveness and rationality of the model were verified through case analysis [5]. Mitiche *et al.* analysed electromagnetic interference (EMI) frequency scans to detect frequencies associated with these faults. These time-resolved signals of key frequencies provided important information for fault type identification and trend analysis. They developed an end-to-end fault classification method based on real-world EMI time-resolved signals. The results demonstrated the high classification performance of its computationally efficient inference model [6].

For fault identification and algorithm research, traditional protection devices cannot detect faults. Chandrasekharan *et al.* proposed a new fault detection algorithm to identify faults in photovoltaic arrays and strings. The effectiveness of this algorithm was verified through MATLAB simulation and experiments under various operating conditions of solar photovoltaic power plants [7]. Shi *et al.* developed a deep neural network (DNN) based method for identifying and classifying power system events by utilising real-world measurements of hundreds of phasor measurement units (PMUs) and labels of thousands of events. They proposed a PMU sorting algorithm based on graph signal processing, and then deployed regularisation based on information loading. The results indicated that the combination of PMU-based sorting and information loading-based regularisation techniques helped the proposed DNN method achieve high-precision event recognition and classification results [8]. To further improve the fault identification ability of protection and adaptive reclosure, Hou *et al.* proposed a hybrid multi-terminal

high-voltage DC system fault identification scheme based on control and protection coordination strategies. In the adaptive reclosing stage, an active fault identification scheme based on the distribution of injected signal amplitude along the line was proposed. Simulation studies showed that this fault identification scheme identified fault areas in various fault scenarios [9]. Liang *et al.* used an improved metaheuristic technique called the developed African vulture optimisation algorithm to provide optimal results for cold, hot, and electric joint systems. The results indicated that, without considering the system, the total cost of purchasing electricity was equal to 420,959 per year, and the cost function value was positive, indicating that the system had a positive effect in reducing system costs [10]. Verrax *et al.* proposed a parameter single-ended fault identification algorithm. It used a short observation window to determine if there was a fault in the circuit monitored by the relay. Combining phenomenological and behavioural aspects to represent fault propagation, considering ground effects and various losses, the fault line was identified based on the size of the estimated confidence region obtained. The performance of this algorithm in a three-node grid was simulated and studied [11].

This study utilised an improved metaheuristic technique, the African vulture optimisation algorithm, which provides a new optimisation tool for similar studies. Although this study has achieved positive results, its scenario setting may be too simplistic, and practical applications require consideration of more factors and conditions. This provides direction for future research. Gao *et al.* proposed a new optimised hybrid renewable energy system (HRES) layout for power supply in remote areas of Türkiye. The final simulation showed that the proposed method provided lower NPC and LCOE compared to other methods [12]. This study not only focuses on system cost and reliability but also considers the impact of supply loss probability on system performance, making the optimisation results more accurate and dependable. To solve the problem of price uncertainty in the electricity market, Cai *et al.* proposed a new mathematical model using a mixed robust stochastic method, aiming to maximise the expected profit of compressed air energy systems. The research results indicated that considering the maximum capacity of cave explorers with uncertainty, under the robustness strategy, the total profit was reduced by approximately 8.68% [13]. This emphasises the importance of considering the uncertainty of the electricity market and provides an effective mathematical model to handle this uncertainty, thereby improving the efficiency and stability of the power system.

In summary, scholars have conducted many algorithmic studies on fault analysis and identification positioning, but the research on multi-scenario, multi-objective, and power grid planning is not yet in-depth enough. Mei *et al.* proposed a stochastic optimal operation model based on multi-scenario simulation, but the model did not include power grid planning. Mitiche *et al.* analysed EMI frequency scans to detect frequencies associated with these faults. Chandrasekharan *et al.* proposed a new fault detection algorithm to identify faults in photovoltaic arrays and strings, but no further optimal grid planning was carried out. Martínez and Cruz-Mendoza used a linear programming optimisation method combined with computational strategies to optimise reading and processing calculations, but the algorithm was cumbersome, and the results needed further conversion. Based on the above research, this study proposes a multi-scenario power system cascading fault identification and power grid planning optimisation scheme based on fault data and state search, which improves the compatibility and adaptability of the power system in different scenarios and maintains the optimal operation state of its line system.

3. Network Method and Power Grid Optimisation Design Based on Multi-Scenario Composite State Faults

With the development of the economy, to meet more power supply needs, it is necessary to expand the power system. However, there are cascading faults and safety issues during the operation of the power grid. Therefore, research is conducted on identifying faults based on the data generated during faults and corresponding states, and multi-objective algorithms are combined to achieve power system fault identification and analysis in multiple scenarios. Therefore, a power system cascading fault identification and power grid optimisation design considering multiple scenarios are proposed.

3.1 Chain Faults Identification and Analysis in Power Systems Based on Fault Data and State Search

Chain faults can trigger major power system outages, causing serious economic losses to society. The occurrence and propagation of cascading faults in the power system are closely related to the faults of some components in the system. These components are key components of the system and have higher criticality than other components. Once a key component in the power system malfunctions, it will trigger a chain reaction, leading to severe power outages [14]. Therefore, identifying and reinforcing these critical components is crucial as a feasible solution to prevent chain failures and curb their spread. Identifying critical faults and components related to them requires relying on chain fault simulation calculations. Power system cascading failure refers to the occurrence of new events in the power grid in a cascading manner and then further leading to the emergence of new events in a cascading manner. The chain and correlation between events are typical characteristics of such events. One of the characteristics of the accident chain is that "the more accident chain conditions are met, the easier accidents are to occur." Chain failures conform to the basic idea of the above accident chain theory, and the accident chain is an effective tool for characterising chain failures. A method for constructing a state fault network based on fault data is proposed to handle the large amount

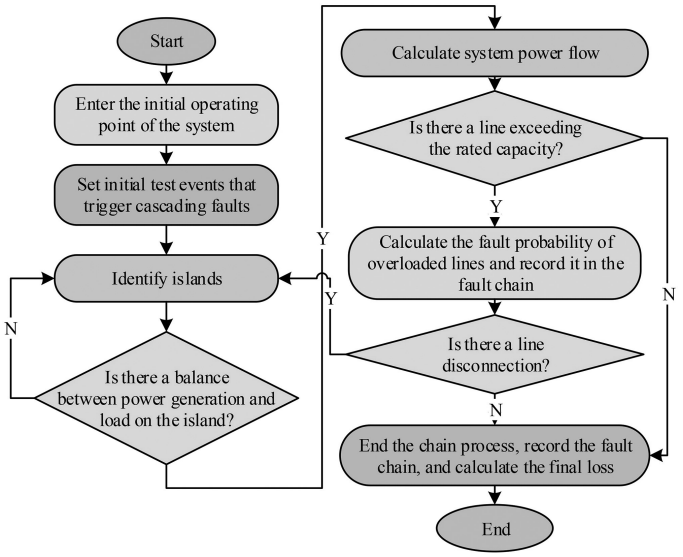

Figure 1. Simulation steps for cascading fault model.

of fault chain data generated during cascading fault simulation, which records the propagation information of such faults [15]. In many simulation models currently developed, transmission line faults have been proven to be the main driving force for propagation, although these faults involve complex processes and factors. Therefore, the focus of the research is to design a simulation model based on DC for generating cascading fault chains. The simulation steps of the cascading fault model are shown in Fig. 1.

The initial operating point of the system is entered, the initial event that triggers the cascading fault is set, and then the fault is identified to balance the power generation load within the fault. The system power flow is calculated to determine if it exceeds the rated capacity. If it exceeds the rated capacity, the fault probability is calculated according to (1) and it is included in the fault chain. If it does not exceed the rated capacity, the interlocking process will end. The fault chain is recorded, and the total loss of the fault chain is calculated [16].

$$\mathrm{Pr}_l^{\mathrm{trip}} = \begin{cases} 1, p_l \geq p_l^{\max} \\ \frac{p_l - p_l^c}{p_l^{\max} - p_l^c}, p_l^c < p_l < p_l^{\max} \\ 0, p_l \leq p_l^c \end{cases} \tag{1}$$

In (1), p_l represents the current transmission power of the line l, p_l^c represents the rated transmission power of the line l, and $p_l^{\max}$ represents the transmission power limit of the line l. The data in the fault chain are reconstructed and analysed, with a system consisting of n components. $\left\{f_{(1)}, \ldots, f_{(k)}\right\}$ represents the recorded fault chain with a length of k, and $f_{(k)}$ represents the number of the faulty component. Using a vector with dimension $1 \times n$ to represent the current operating state of the system, 0 represents the component in operation, and 1 represents the component out of service [17]. If the initial state of the system is denoted as s_0, then there is $s_0 = 0^{1\times n}$, and $k+1$ system states are obtained from this fault chain, denoted as $\{s_0, s_1, \ldots, s_k\}$. Then, pair the state with the corresponding faults in the fault chain to form a binary sequence, denoted as $\left(s_0, f_{(1)}\right), \left(s_1, f_{(2)}\right), \ldots, \left(s_k, f_{(0)}\right)$. After pairing faults and states, a binary can specifically indicate the location of the faulty component. Figure 2 shows the fault chain information recorded by a system containing six lines.

$N_{k,s}$ and $N_{k,f}$ are the states located in the k fault stage and the number of faults, respectively, $s_{k(j)}$ represents the j state located in the k fault stage. From this, a binary is obtained, which is the part represented in blue in Fig. 2. By processing fault chain data, the network structure of state faults is obtained [18]. Next, the state and fault values are calculated, denoted as S and F, respectively.

For S values, $s_{k(j)}$ is set and the possible faults f_l are known, and their S values are calculated as shown in (2).

$$\begin{cases} S\left(s_{k(j)}\right) = \sum\limits_{f_l \in S_{s_{k(j)}}} \frac{N_{\left(s_{k(j)}, f_l\right)}}{N_{s_{k(j)}}} F\left(s_{k(j)}, f_l\right) \\ N_{s_{k(j)}} = \sum\limits_{f_l \in S_{s_{k(j)}}} N_{\left(s_{k(j)}, f_l\right)} \end{cases} \tag{2}$$

In (2), $N_{\left(s_{k(j)}, f_l\right)}$ represents the number of f_l occurrences of the $s_{k(j)}$ state and $N_{s_{k(j)}}$ represents the number of occurrences of the $s_{k(j)}$ state recorded in the fault data. For the calculation of F values, since the loss data of cascading faults is introduced into the state fault network by f_0, the F value of f_0 is equal to the final loss of the recorded fault chain. For the actual faults of other components, the value is equal to the value of the state it points to, as shown in (3).

$$\begin{cases} F\left(s_{k(j)}, f_0\right) = L, f_0 \in S_{s_{k(j)}} \\ F\left(s_{k(j)}, f_l\right) = S\left(s_{k+1(i)}\right), f_l \in S_{s_{k(j)}}, f_l \in S^{\mathrm{pf}}_{s_{k+1(j)}} \end{cases} \tag{3}$$

In (3), f_l represents the actual fault of other components. The load loss of all fault chains in this system, such as the F value of terminal state, is shown in Fig. 3.

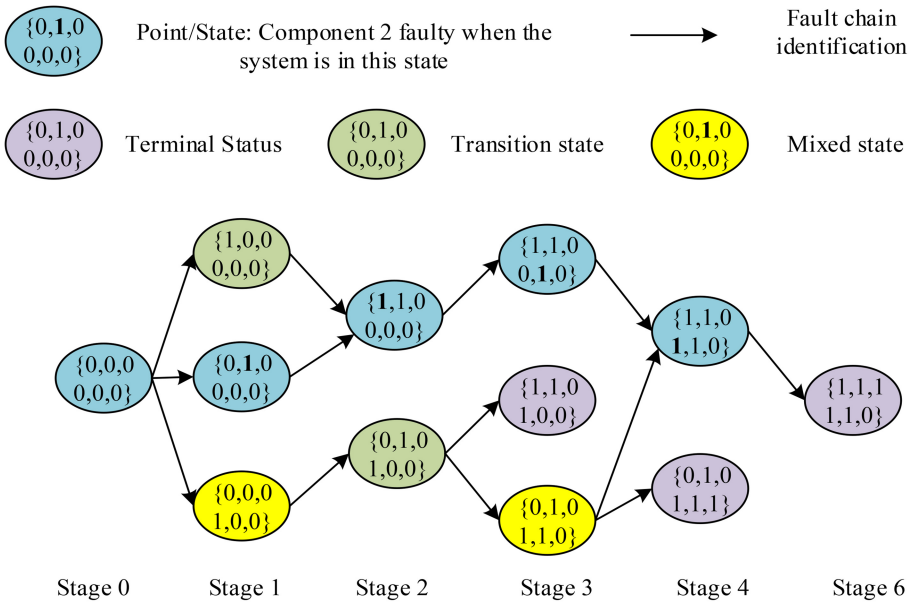

Figure 2. Fault chain information recorded by the system for six lines.

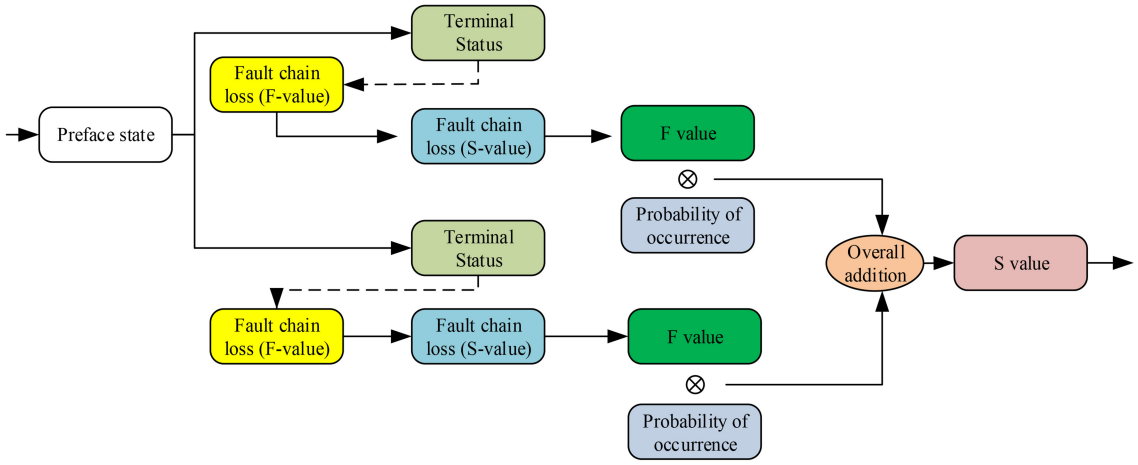

Figure 3. The load loss of all fault chains in this system, such as the value of terminal state.

The S value can measure the risk of cascading failures of the system in that state. Therefore, different F values in the state fault network can be used to identify key components of the system. The S value of a state quantifies the risk of cascading faults in the system in that state, while the F value of a fault indicates the risk of cascading faults in the system after the occurrence of that fault [19]. Figure 4 shows the process of identifying critical faults in a state fault network.

In Fig. 4, the green part represents the initial fault, while the blue circle represents a situation that only contains one possible fault. In the second stage, the blue arrow indicates that faults with a state fault network F value that is not higher than the state S value need to be eliminated, while the black arrow indicates faults with a F value higher than the state S value that need to be retained. The key faults identified in the third stage are recorded as $\left(a, f_{a(2)}\right), \left(b, f_{b(1)}\right), \left(b, f_{b(3)}\right), \left(c, f_{c(2)}\right)$. In the risk calculation of chain failures, over 70% of system interference and fault prevention are related to hidden failures. The occurrence of hidden faults is affected by exposure, and further research defines the state as a sequence of fault lines with cascading faults [20], as shown in (4).

$$s_k = \left[f_{(1)}, f_{(2)}, \ldots, f_{(k)}\right] \tag{4}$$

In (4), s_k represents the state of k faulty line. To avoid the influence of sampling randomness, the system's cascading fault risk calculation is adopted in the improved state fault network [21]. Equation (5) calculates the sum of losses generated by various stages of the state.

$$z_i = \breve{z}\left(s_1^i\right) + \breve{z}\left(s_2^i\right) + .. + \breve{z}\left(s_k^i\right) \tag{5}$$

In (5), z_i represents the final recorded power outage loss of the i fault chain, $\breve{z}\left(s_k^i\right)$ is the load loss generated at the state s_k^i. Substituting (5) into (4) yields (6).

$$r = \frac{1}{N_M}\sum_{i=1}^{N_M}\left(z\left(s_1^i\right) + z\left(s_2^i\right) + \cdots + z\left(s_k^i\right)\right) \tag{6}$$

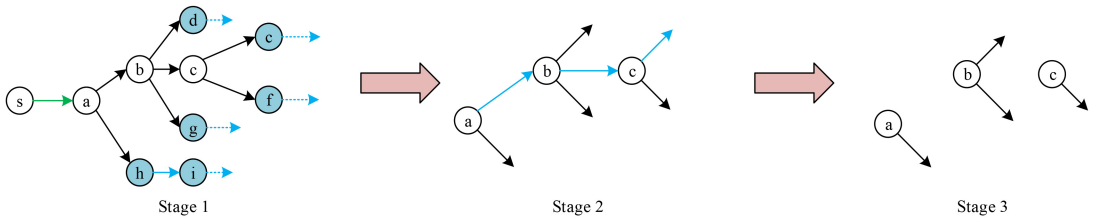

Figure 4. Key fault identification steps in state fault networks.

The accurate assessment of the risk of cascading faults can be represented by the sum of the risks of all states in the state fault network, as shown in (7).

$$r = \sum_{j=1}^{N_1^s} \Pr\left(s_{1(j)}\right) \breve{z}\left(s_{1(j)}\right) + \sum_{j=1}^{N_2^s} \Pr\left(s_{2(j)}\right) \breve{z}\left(s_{2(j)}\right) + \cdots + \sum_{j=1}^{N_k^s} \Pr\left(s_{k(j)}\right) \breve{z}\left(s_{k(j)}\right) + \cdots \tag{7}$$

In (7), $\Pr\left(s_{k(j)}\right)$ represents the probability of convergence to the corresponding state as the total number of simulation samples N_M increases. It is necessary to evaluate the consequences of various possible faults in advance to guide the direction of state search and introduce risk assessment indicators. The research mainly considers calculating two factors: fault probability and fault loss. The probability of a possible fault occurring on a certain line in a certain state can be directly obtained through implicit fault probability and overload fault probability, as shown in (8).

$$\begin{cases} \Pr\left(s_{k(j)}, f_l\right) = \Pr^H\left(s_{k(j)}, f_l\right) + \Pr^F\left(s_{k(j)}, f_l\right) \\ \begin{cases} \Pr^H\left(s_{k(j)}, f_l\right) = p_l^{\mathrm{HW}} \\ \Pr^F\left(s_{k(j)}, f_l\right) = p_0^{\mathrm{HW}} p_l^{\mathrm{FW}} \end{cases} \\ \Pr_0\left(s_{k(j)}, f_l\right) = p_0^{\mathrm{HW}} p_0^{\mathrm{FW}} \\ \Pr\left(s_{k+1(j')}\right) = \Pr\left(s_{k(j)}\right) \Pr\left(s_{k(j)}, f_l\right) \end{cases} \tag{8}$$

In (8), l represents the line, $s_{k(j)}$ represents the state, $\Pr_0\left(s_{k(j)}, f_l\right)$ represents the probability of no fault occurring, and $\Pr\left(s_{k+1(j')}\right)$ represents the probability of its subsequent state $s_{k+1(j')}$ when the fault is disconnected during the search process. Regarding the calculation of fault losses, the research evaluates the impact of faults through system splitting losses and line overload losses. Based on the two factors of fault probability and fault loss mentioned above, the fault risk assessment indicators for the line are shown in (9).

$$\rho\left(s_{k(j)}, f_l\right) = \Pr\left(s_{k(j)}, f_l\right) \sigma\left(s_{k(j)}, f_l\right) \tag{9}$$

In (9), $\sigma\left(s_{k(j)}, f\right)$ represents the fault loss. After simulation calculation, the information is stored in the state fault network. Record faults in the same state and directly re read them when encountering them again to avoid repeated consumption. The entire search process is shown in Fig. 5.

3.2 Composite State Fault Analysis and Power Grid Planning Optimisation Considering Multiple Scenarios

The operating status of the power system is not fixed and will include different operating scenarios with significant differences throughout the year. Therefore, the analysis method for a single scenario is not sufficient to meet the needs of actual power grid operation analysis. Meanwhile, chain failures may also develop in different scenarios through different propagation paths. Therefore, multi-scenario analysis for risk control of chain failures is of great significance. The previous section discussed in depth the analysis methods based on fault data, but the current analysis methods based on fault data are not suitable for multi-scenario analysis. The method developed by this research institute is called the state fault network, which can detect critical power lines in a single operating scenario and integrate and analyse fault data generated by various operating modes [22]. However, its design cannot distinguish between multiple scenarios. Although specific scenario analysis can be conducted through separate calculations and evaluations to draw comprehensive conclusions, there are no specific connections or significant differences between different scenarios. Therefore, a composite state fault network method considering multi-scenario and multi-objective optimisation has been proposed. The improved state fault network method can balance the analysis needs of multiple scenarios while utilising the computational efficiency of the composite state fault network method to quickly calculate multi-scenario multi-objective optimisation problems in power systems. The power system operates throughout the year, and the maintenance plan significantly changes its operating mode. There are significant differences in the probability of faults and power outages of system lines under different operating modes. To process fault data and generate a state fault network, it is necessary to distinguish the source of fault data.

The number of times the $s_{k(j)}$ state has occurred and the number of possible faults are recorded, and the F values of possible faults and their own S values in the record are calculated. In multiple scenarios, fault chain data are recorded into states and then the source of the current scenario is distinguished. The schematic diagram of the composite state fault network is shown in Fig. 6.

The improved state fault network consists of multiple scenarios, $s_{k(j)}$ is set as one of the composite states, and the S values are calculated in the scenario as shown

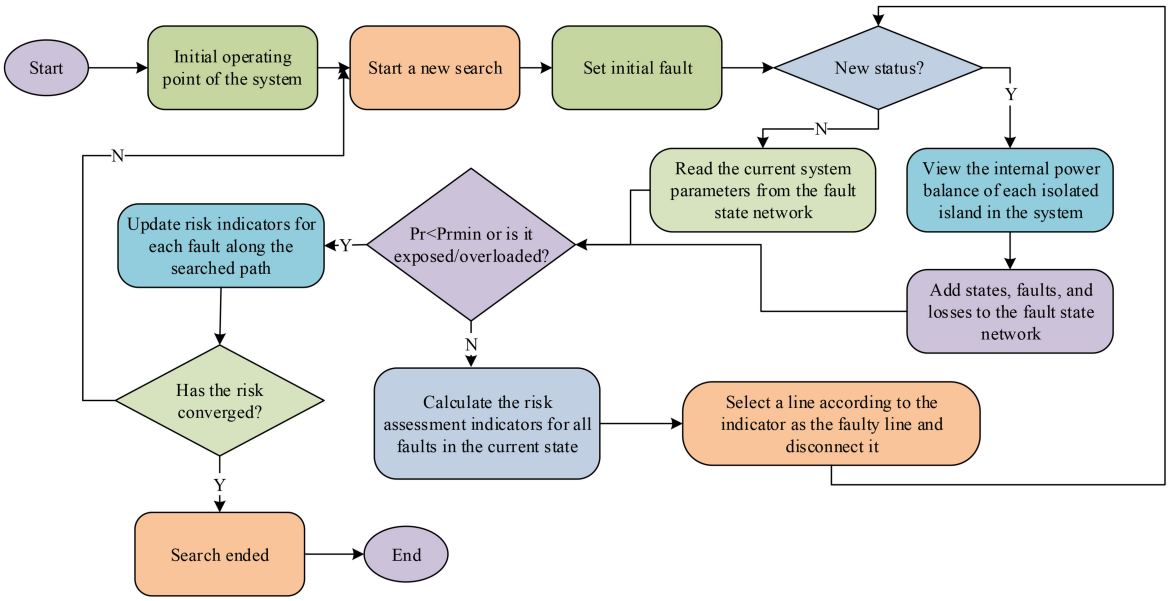

Figure 5. Flowchart of state fault network search.

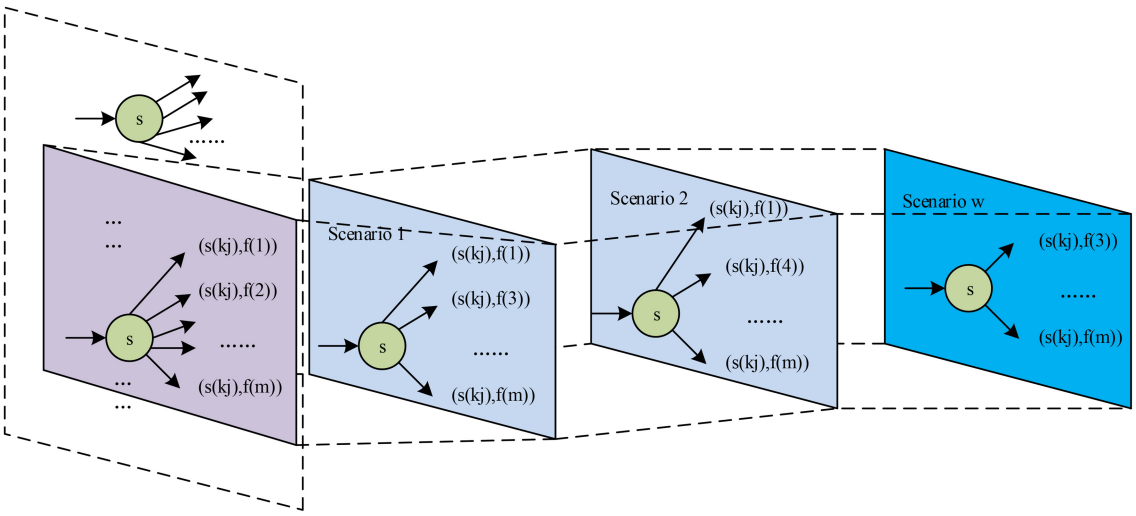

Figure 6. Schematic diagram of composite state fault network.

in (10).

$$S^{w}\left(s_{k(j)}\right)=\sum_{f_m\in S^{w}_{s_{k(j)}}}\frac{N^{w}_{\left(s_{k(j)},f_m\right)}}{N^{w}_{s_{k(j)}}}F^{w}\left(s_{k(j)},f_m\right)\quad(10)$$

In (10), $S^{w}\left(s_{k(j)}\right)$ represents the S value of the w scenario corresponding to the $s_{k(j)}$ state, $F^{w}\left(s_{k(j)},f_m\right)$ represents the value of the F fault in the w scenario corresponding to the $s_{k(j)}$ state, $N^{w}_{s_{k(j)}}$ and $N^{w}_{\left(s_{k(j)},f_m\right)}$ represent the number of $s_{k(j)}$ occurrences of the states $s_{k(j)}$ and f_m recorded in the fault data from the w scenario. If the fault chain in the w scenario ends in $s_{k(j)}$ state, the F value of f_0 is recorded in the w scenario.

In terms of composite state fault networks, the calculation and analysis at the overall level need to pay attention to the statistics of all scenario information. Under the requirements of distinguishing storage and calculation, the composite S values and composite F values of each state and fault can be calculated at the overall level. Assuming that the S values of the $s_{k(j)}$ state are known in each scenario, the load S value and composite F value of the $s_{k(j)}$ state are calculated as shown in (11).

$$\begin{cases}S\left(s_{k(j)}\right)=\dfrac{\sum\limits_{w=1}^{N_c}N^{w}_{s_{k(j)}}S^{w}\left(s_{k(j)}\right)}{\sum\limits_{w=1}^{\mathrm{Nc}}N^{w}_{s_{k(j)}}}\\ N_{s_{k(j)}}=\sum\limits_{w=1}^{\mathrm{Nc}}N^{w}_{s_{k(j)}}\\ F\left(s_{k(j)},f_m\right)=\dfrac{\sum\limits_{w=1}^{\mathrm{Nc}}N^{w}_{\left(s_{k(j)},f_m\right)}F^{w}\left(s_{k(j)},f_m\right)}{\sum\limits_{w=1}^{N_c}N^{w}_{\left(s_{k(j)},f_m\right)}}\end{cases}\quad(11)$$

In (11), N_c represents the total number of scenarios considered. The total number of state occurrences in a composite state fault network and the number of

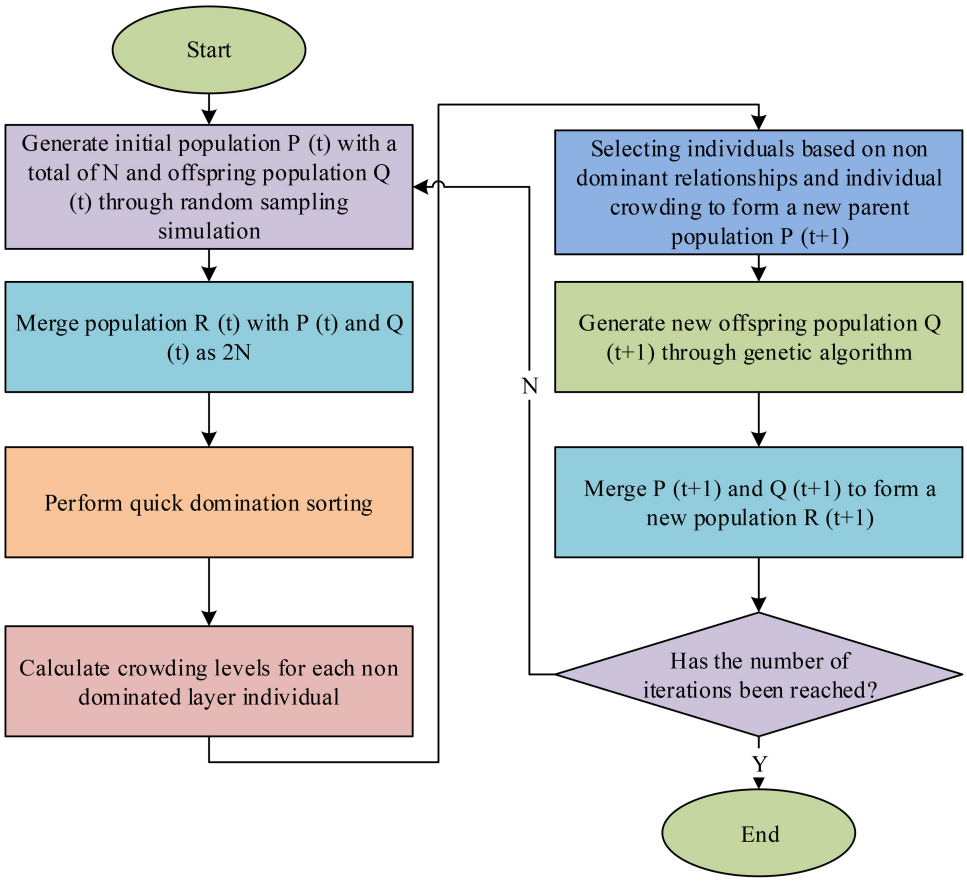

Figure 7. NSGA-II algorithm basic thinking flowchart.

occurrences in different scenarios satisfy (11). The relationship between composite F values and composite S values is shown in (12).

$$S\left(s_{k(j)}\right)=\sum_{f_m\in\bigcup_{w=1}^{N_c}S_{k(j)}^{w}}\frac{\sum_{w=1}^{N_c}N_{\left(s_{k(j)},f_m\right)}^{w}}{\sum_{w=1}^{N_c}N_{s_{k(j)}}^{w}}F\left(s_{k(j)},f_m\right) \tag{12}$$

Compared to a single scenario running mode, multi-scenario optimisation problems typically require consideration of the optimisation objectives of each scenario. In the optimisation problem of multi-scenario line expansion, the objective function at least includes the expansion construction cost and the overall risk of chain failures throughout the year. As the number of scenarios increases, it is also necessary to consider controlling the risk of chain failures in peak load scenarios throughout the year. In multi-objective problems with multiple scenarios, optimising one objective may result in the loss of other objectives as a cost [23]. Therefore, the concept of Pareto optimal solution is introduced in the study. The Pareto frontier includes the combination of different optimisation objectives, which can meet the different preferences for each optimisation objective. In addition, the NSGA-II algorithm is used to solve the Pareto optimal set. NSGA-II introduces fast-dominated sorting, crowding degree, and elite strategy to determine operators, reducing algorithm complexity, and making the Pareto optimal solution uniformly extend to the entire Pareto frontier. The basic idea flowchart of the NSGA-II algorithm is shown in Fig. 7.

Consider improving the state fault into a multi-scenario composite state fault network, achieving multi-scenario multi-objective optimisation of the composite state fault network, for rapid assessment of cascading fault risk in multi-scenario scenarios. The expansion line is det as $l_1, l_2, \ldots, l_k$, the expansion capacity is $u_1, u_2, \ldots, u_k$, denoted as $l=[l_1, l_2, \ldots, l_k]^T$, $u=[u_1, u_2, \ldots, u_k]^T$. (u, l) represents a line expansion plan. Assuming that the line expansion cost of the system is positively correlated with the expansion capacity, the expansion cost is set to $c_1, c_2, \ldots, c_k$, and the expansion unit price vector is $c=[c_1, c_2, \ldots, c_k]^T$. The economic cost function of the expansion plan is shown in (13).

$$C\left(u,l\right)=c^{T}u \tag{13}$$

After expanding the system according to the plan, the scenario $G=\{w_1, \ldots, w_g\}$ is set as the scenario of peak load mode. Based on the composite state fault network, the annual change in chain fault risk, *i.e.*, the degree of risk reduction, and the corresponding scenario of chain fault risk reduction, are calculated, as shown in (14).

$$\begin{cases} R\left(u,l\right)=\frac{r(u,l)}{r(0,l)} \\ R^{G}\left(u,l\right)=\frac{r^{G}(u,l)}{r^{G}(0,l)} \end{cases} \tag{14}$$

In (14), $r^G(u,l)$ represents the multi-scenario cascading fault risk calculated based on the composite state fault network after applying the expansion plan. In summary, the optimisation problem modelling with (13) and (14) as objective functions are shown in (15).

$$\begin{aligned} &\min\left(C(u,l), R(u,l), R^G(u,l)\right) \\ &s.t. \quad 0 \le u_k \le \alpha_k \\ &C(u,l) < C_{\max} \end{aligned} \tag{15}$$

In (15), $C_{\max}$ is the upper limit of the total system expansion cost, α_k represents the maximum expansion capacity of the line l_k. The current multi-scenario modelling technique suffers from slow efficiency, so the study uses a simulated annealing algorithm with better robustness to optimise it in the following steps. First, the power system failure parameters are initialised, *i.e.*, expansion cost and expansion capacity, and then the step factor for controlling the generation of new solutions is searched. The difference in the objective function between the new solution and the current solution is calculated, and the Metropolis criterion is used, *i.e.*, worse new solutions are accepted according to a certain probability to increase the search space. When the termination condition is reached, the algorithm ends, and the optimal solution is returned.

4. Network Method Simulation Experiment for Fault Analysis of Multi-Scenario Power Systems

To achieve cascading fault analysis and power grid planning in multiple scenarios, a fault identification method based on fault data and state search was studied and analysed. The multi-objective algorithm NSGA-II was combined to solve the Pareto optimal set and achieve fault identification and analysis. A simulation experiment was designed for verification.

4.1 Experimental Data and Design

The experimental dataset was sourced from the annual operating condition records of a power system with 18,234 fault chain data volume, which contained 48 branch circuits with a load of 6,274.53 MW. The system loss was measured by the total outage load volume and was numerically divided by the total system load volume to normalise it. The initial faults were random N-2 faults. The co-channel interference (CCI) was updated every 500 fault chains, and the change in CCI was detected as shown in Fig. 8. The dashed line represented the convergence threshold ε. Convergence threshold was taken 0.0005, CCI reached the convergence condition when there were 15,590 fault chain data, so the state fault network generated by 15,590 fault chains was used to calculate CCI.

When the system was running, MATLAB was used to write a testing program, and all loads of the operating parameters were increased by 1.5 times. For the results of critical line identification, the effectiveness of critical line identification was verified by expanding the critical lines, counting the risk of the system after expansion, and comparing the level of risk reduction. All lines were

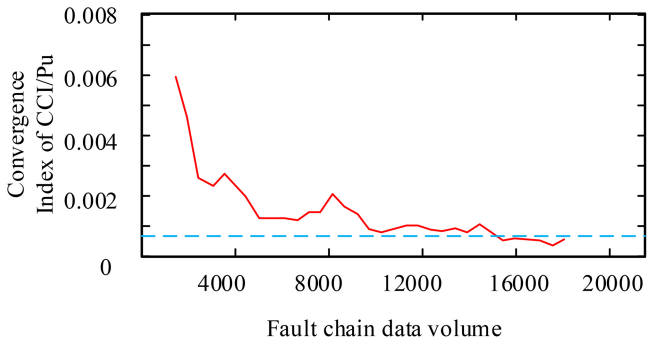

Figure 8. CCI variation chart of IEEE node system.

Table 1
The Five Most Critical Paths Identified by EB, CFG, and State Fault Network Methods

Serial number	EB	CFG	State fault network
1	25 (13-14)	29 (17-27)	3 (6-7)
2	29 (15-16)	20 (12-32)	44 (26-27)
3	3 (6-7)	37 (15-34)	34 (13-24)
4	29 (16-19)	49 (25-31)	13 (12-25)
5	31 (25-26)	5 (5-14)	8 (9-15)

arranged in descending order of CCI, and three groups of lines were selected, each group contained five lines, and three groups of lines were listed. The three groups of lines with a significant gap in CCI in magnitude were selected, and a CCI of 0 indicated that there may have been no failures in these lines, or the failures that occurred were not critical failures. So, three groups of lines were selected in the system for chain fault simulation after expansion, and the risk of chain faults was counted and compared with the risk profile of the original system. The initial fault event was a random N-0 fault. To verify the effectiveness of the state fault network method, its recognition results were compared with the extended betweenness (EB) method and the cascading failure graph (CFG) method. The five most critical paths identified by EB, CFG, and state fault network methods are shown in Table 1.

To explore scenarios with multiple scenarios, the research design considered four load levels based on four seasons: spring, summer peak, autumn, and winter peak. Four basic scenarios were set throughout the year, with a proportion of 0.25, and each scenario had an equal duration throughout the year.

The power system under study contained 5,000 nodes and 20,000 lines spread over several regions and countries. The nodes included power plants, substations, transmission lines, and distribution systems. The system involved multiple types of equipment, such as gas turbines, hydroelectric power, nuclear power generation, *etc.* It also included multiple modes of operation, such as normal operation, emergency standby, and maintenance. The experiments were designed with multiple complex

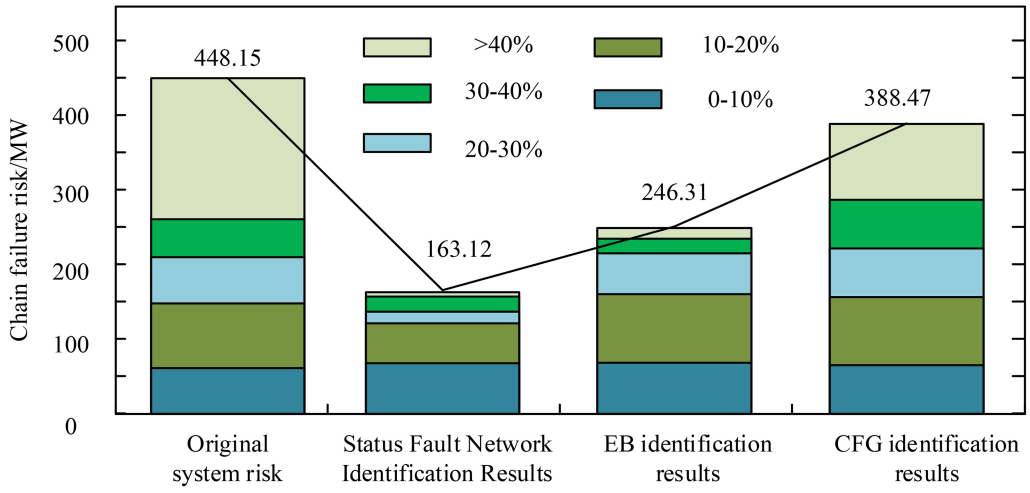

Figure 9. Comparison of different methods for identifying the risk of chain failures after key line expansion in IEEE39 node system.

fault scenarios, including multiple faults, interlocking faults, and faults in interruption mode. For example, simultaneous multiphase short circuits, a series of chain reactions triggered by internal transformer faults, *etc.* The robustness of the study, *i.e.*, stability and reliability under different environments and conditions, was also evaluated.

4.2 Measurement and Analysis of Experimental Results

Figure 9 shows a comparison of the risk of cascading faults after identifying key line expansion using different methods. There were significant differences in the most critical lines identified by the three methods. After expanding the lines identified by the state fault network method, the risk of cascading faults in the system decreased from 448.15 MW to 163.12 MW, the EB method decreased to 246.31 MW, and the CFG method decreased to 388.47 MW. The method proposed by the expansion research institute effectively reduced the risk of chain failures by identifying key routes. In this experimental phase, 15,590 fault chains were simulated and the state fault network was updated 29 times, taking a total of 101.68 s. The simulation took 95.94 s, which was 94.35% of the total time. The update status of the faulty network took 5.74 s, with an average update time of 0.197 s. The visible state fault network method had high computational efficiency.

In Fig. 9, a faulty circuit was selected for the experiment to compare the risk of using the state fault network and Monte Carlo simulation. Figure 10(a) shows that the risk calculated by Monte Carlo sampling simulation ultimately converges to the risk value of 207.14 MW calculated by the state fault network. The construction of a state fault network took 4,618.10 s, while the Monte Carlo sampling simulation took 7,694.79 s under the same conditions, indicating that the calculation time for searching and constructing a state fault network was better. As the research focused more on searching for increasingly complete hidden fault events, the statistical data of the changes in the number of hidden faults in the new sampling of the two methods are shown in Fig. 10(b). Figure 10(b) shows the statistical changes in the number of hidden faults newly sampled by two methods. The number of new hidden faults collected by Monte Carlo sampling simulation was only 4.7% of the search state fault network method. Therefore, the search state fault network method proposed in the study performed good at capturing as complete a set of hidden fault events as possible.

In multiple scenarios, key routes were selected for route expansion in the experiment, and the routes ranked lower throughout the year were expanded. The distribution of the solutions showed that as the cost of line expansion increased, the overall chain failure risk for the whole year and the chain failure risk for the winter peak scenario tended to decrease. In Fig. 11(a), a black dot represents a nondominated solution. Since the Pareto front hardly changed after iterative optimisation up to 40 generations, the nondominated solutions of the 45th to 50th generations were superimposed on the graph and fitted to obtain the surface for the sake of accurate surface fitting. Figure 11(a) shows the optimal solution set for multi-scenario multi-objective optimisation, where the total capacity of the line expansion gradually decreased to 600 megawatts, resulting in a reduction in the Pareto front. The overall risk of chain failures throughout the year gradually decreased to 66% as the total cost of line expansion increased, while chain failures during winter peak hours decreased to 72%. To make it more convenient to view, the experiment rotates Fig. 11(a) into an elevation view as a plot of the relationship between the overall annual risk and the winter peak risk, as shown in Fig. 11(b). Figure 11(b) shows the relationship between overall risk throughout the year and winter peak risk. There was a negative correlation between overall risk throughout the year and winter peak scenario risk under fixed expansion costs. This suggested that system planners needed to strike a suitable balance between the two when considering expansion scenarios if they did not have a particular risk appetite.

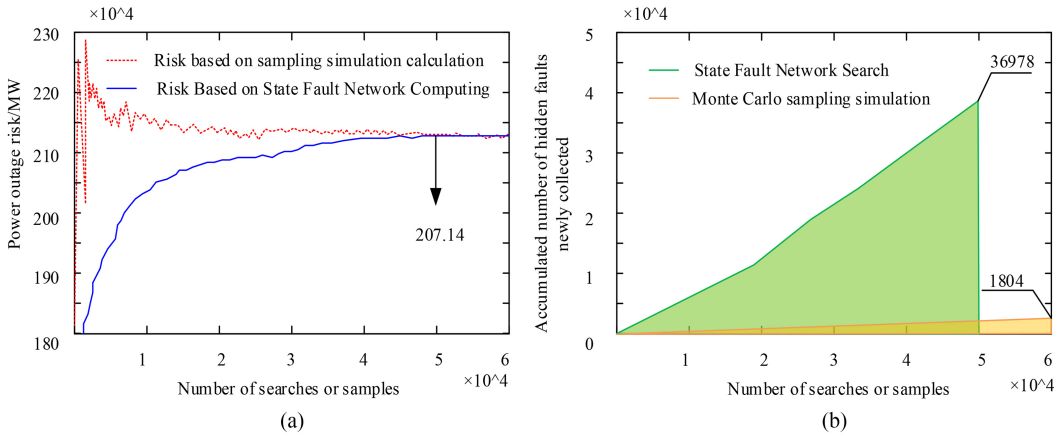

Figure 10. Risk comparison of state fault networks and Monte Carlo simulation: (a) comparison of cascading fault risks in IEEE118 node systems and (b) the relationship between the cumulative number of newly collected hidden faults and the number of searches.

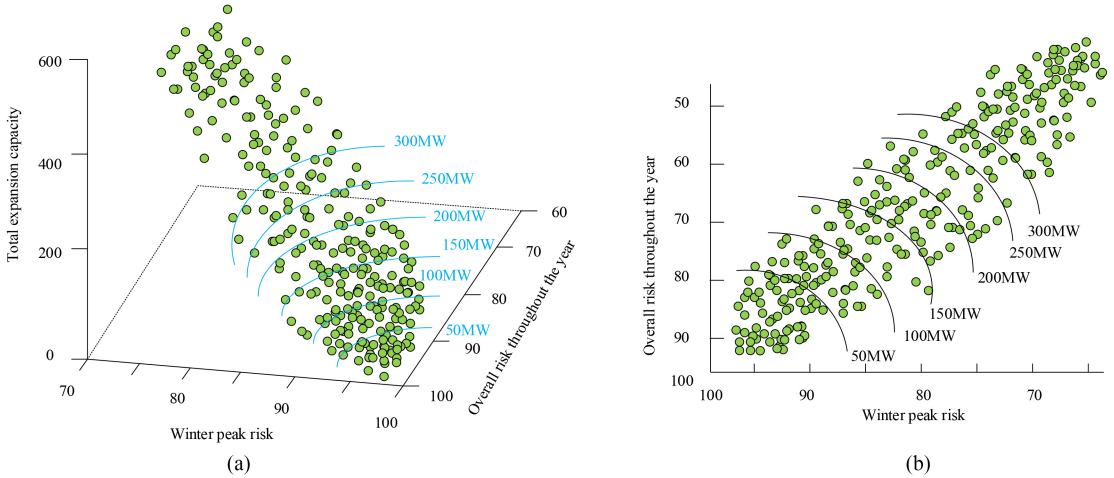

Figure 11. Cost of line expansion for key lines, overall risk throughout the year, and risk situation during winter peak scenarios: (a) IEEE39 node multi scene multi objective optimisation optimal solution set and (b) plane projection of the optimal solution set for IEEE39 node multi scene multi objective optimisation.

Table 2 shows the selected sets of optimal solutions and their degree of risk reduction in the multi-scenario multi-objective optimisation optimal solution set. In Table 2, except for line 8, which has almost the same expansion capacity, and lines 36 and 42, which do not have much difference in expansion capacity, lines 40 and 95 have a very significant change in contrast. For line 8, after the total expansion capacity exceeded 35 MW, the line reached the limit of expansion utility. For lines 36 and 42, they were not significantly allocated expansion capacity as they were less critical than lines 40 and 95 under scenarios 1 and 3, respectively. Regarding the critical line 40 under Scenario 1, the sequence of points A, B, and C indicated that as the expansion capacity of line 40 increased within the total expansion capacity, the risk decreased for Scenario 1 and increased for Scenario 3. The opposite was true for the more critical Line 95 under Scenario 3. Lines 40 and 42 had lower criticality, therefore the allocated expansion capacity was minimal. In the degree of risk reduction in each scenario, the calculation results of the composite state fault network were similar to those of Monte Carlo sampling. In terms of computational efficiency, it took about 15 s for a state fault network to calculate the risk of cascading faults, but if NSGA-II relied on Monte Carlo simulation for calculation, it increased the time consumption by about 110 times. From this, the accuracy of the state fault network was similar to that of the Monte Carlo method, but it had faster computational efficiency.

To verify the stability of the algorithm in different scenarios, an interrupt mode, namely, Scenario 4, was added to statistically analyse the algorithm's detection and recognition rate, as shown in Fig. 12. In interrupt mode, although the recognition rate of the algorithm decreased, it was still around 91%, while in other scenarios, the detection recognition rate of the algorithm remained stable at around 96%.

The study compared the accuracy and error values of the current multi-scenario power system cascading fault identification algorithm with particle swarm optimisation (PSO) and differential evolution algorithm (DE), as shown

Table 2
Several Sets of Optimal Solutions Selected in the Multi-Scenario Multi-Objective Optimisation Optimal Solution Set and Their Degree of Risk Reduction

/		A	B	C
Whole	State fault network	65.24%	61.54%	59.14%
	Monte Carlo sampling	65.44%	62.48%	57.94%
Scenario 1	State fault network	75.84%	72.18%	68.25%
	Monte Carlo sampling	74.25%	73.16%	67.11%
Scenario 2	State fault network	61.78%	58.34%	55.84%
	Monte Carlo sampling	59.48%	59.17%	54.28%
Scenario 3	State fault network	44.18%	50.46%	57.49%
	Monte Carlo sampling	45.94%	49.12%	55.87%
Line	8	38.54	37.99	37.48
	40	7.94	28.48	51
	36	1.15	4.25	3.28
	42	3.48	2.34	2.77
	95	52	21.05	0
Expansion capacity		94.57	92.48	92.34

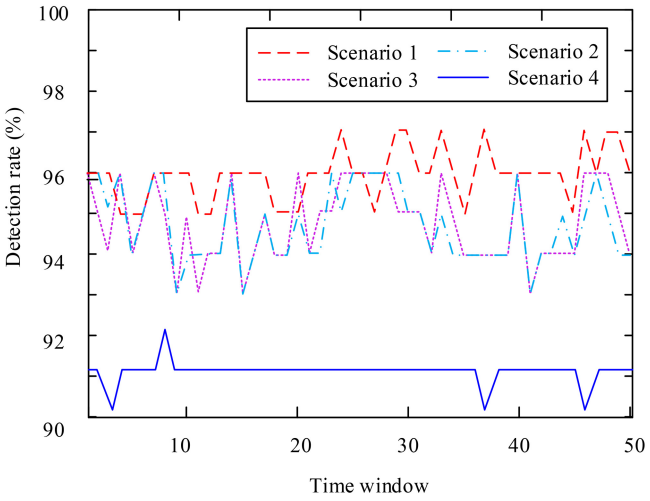

Figure 12. Comparison of fault recognition data detection rates in different scenarios.

in Fig. 13. The accuracy of the research algorithm was always higher than PSO and DE, and the error was also lower than the other two evolutionary algorithms, with the best values of 0.958 and 0.013, respectively.

To thoroughly evaluate the algorithm performance during the interruption and in cross scenarios, a study was conducted on 12 different types of power lines in different parts of the power system. After the partial interruption of the circuit system where the lines were located, fault identification algorithms were implemented. The first six types were the lines in Scenario 1, and the last six types were the lines in Scenario 2. The search for fault time and power system recovery time is shown in Fig. 14. Fault recognition algorithms in different scenarios can quickly find and accurately restore the operation of the power system.

The study introduced a state fault network method that utilises fault data to improve the accuracy of fault network analysis. By enhancing the state fault network with additional system state parameters, the method was applied to assess the operational risk of the power system. This approach enabled the calculation of the chain fault risk assessment by establishing an analytical relationship between the power system parameters and the state fault network parameters. A composite state fault network method considering multiple scenarios was proposed, which utilised the sampling technology to adaptively adjust the sampling weights according to the characteristics of the scenario-sampled fault chain to improve the generation efficiency of the composite state fault network. At the same time, multiple objectives, such as economic indicators and safety indicators for multi-scenario risks were considered and solved using fast computation of composite state fault networks. The control results of the resulting Pareto-optimal solution set for different scenarios were analysed experimentally to provide more flexible choices for operation planners, while the comparison of the computational results with the corresponding Monte Carlo sampling simulation results verified the accuracy of the proposed method. The research is of realistic and practical significance for improving the security, stability, and economy of the power system and providing dedicated support for the safe and stable operation of the power system.

To successfully implement a big data and multi-objective optimisation-based approach to power system

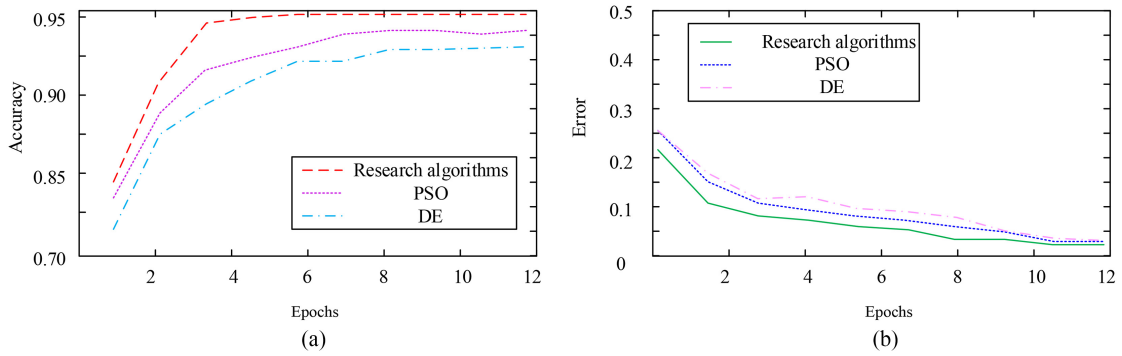

Figure 13. Comparison of precision and error of different evolutionary algorithms: (a) accuracy comparison and (b) error comparison.

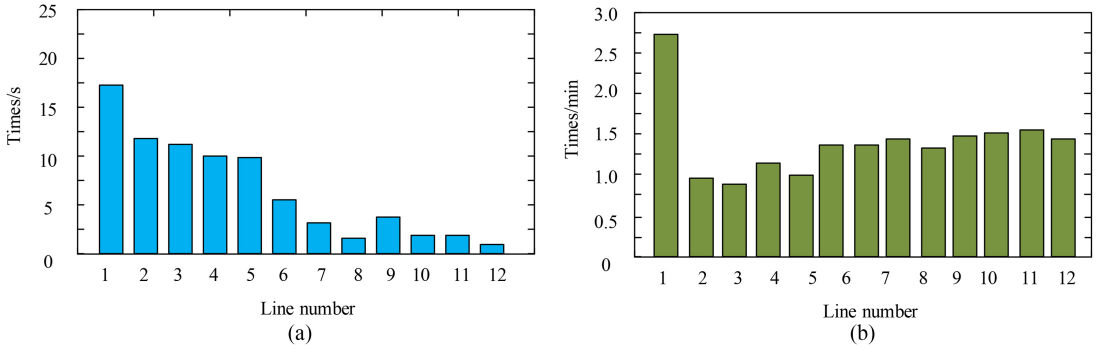

Figure 14. Research on fault identification algorithms for fault identification and power system recovery time in different scenarios: (a) finding fault time and (b) power system recovery time.

fault analysis, organisations need to carefully consider and address aspects, such as data requirements, computational scalability, and practical application barriers. For data quality and integrity, fault data needs to be of high quality and complete for accurate fault identification and analysis. Moreover, as the scale and complexity of the power system increases, the amount of fault data grows dramatically, requiring efficient data processing and storage technologies to cope with large-scale data processing. In terms of computational scalability, large-scale parallel computing requires powerful hardware resources, including high-performance CPUs, GPUs, and storage devices. For practical implementation barriers to institutional adoption, people with appropriate big data and power system expertise and skills are needed in organisations to ensure that the approach is implemented and applied correctly. This may require additional training and recruitment. It should be ensured that all data processing and analysing activities comply with the relevant regulatory and policy requirements, especially regarding data privacy and security.

5. Conclusion

The power system is an essential infrastructure that plays a key role in people's daily lives and socio-economic development. However, with the operation of the power system, there are significant differences in the application and maintenance of multiple scenarios across different periods and environments. The purpose of this study is to improve the multi-scenario compatibility of power system fault analysis by analysing and identifying cascading faults. A composite state fault network method considering multi-scenario and multi-objective optimisation is proposed to solve the Pareto optimal set. Through the application of these methods, the operational risk and cascading fault risk of the system can be more accurately evaluated, resource allocation can be optimised, and the operational efficiency and safety of the power system can be improved. The experiment showed that constructing a state fault network took 4,642.09 s while completing equal sampling in the Monte Carlo sampling simulation took 7,622.80 s. In terms of computational efficiency, relying on a composite state fault network to calculate the risk of cascading faults for NSGA-II took about 15 s. The accuracy of the visible state fault network was similar to that of the Monte Carlo method, but it had faster computational efficiency. As the total cost of line expansion increased, the overall risk of chain failures throughout the year gradually decreased to about 66% before the expansion, while the winter peak decreased to 72%. The proposed method is effective in terms of computational efficiency and risk reduction in multiple scenarios. Although the studied fault identification algorithm for faults needs to rely on historical fault data, the study's optimisation for multiple scenarios improves the compatibility and applicability of fault analysis in different scenarios. although the operating state of the power system may be affected by a variety of factors, resulting in uncertainty in the occurrence of faults. The NSGA-II algorithm's ability to

solve the Pareto optimal set provides a means to balance the conflict between different objectives and optimise multi-objective optimisation problems. Additionally, fault identification through state search is an innovative approach that surpasses traditional parameter-based fault diagnosis methods, allowing for more accurate fault location and cause identification. As a result, this method remains advantageous in addressing uncertainty problems. However, due to technical reasons, there are still some shortcomings in the research, and the load parameters of the line have not been fully addressed, and further exploration is needed in the future.

References

[1] S.R.D. Stallon and M.N. Rajkumar, Improving the performance of grid connected doubly fed induction generator by fault identification and diagnosis: A kernel PCA SMO technique, *International Transactions on Electrical Energy Systems, 31*(4), 2021, e12844.1–e12844.23.

[2] M.R. Rezaei, S.R. Hadian-Amrei, and M.R. Miveh, Online identification of power transformer and transmission line parameters using synchronized voltage and current phasors, *Electric Power Systems Research, 203*, 2022, 107638.1–107638.10.

[3] T. Li, Z. Li, and W. Li, Scenarios analysis on the cross-region integrating of renewable power based on a long-period cost-optimization power planning model, *Renewable Energy, 156*, 2020, 851–863.

[4] M.A. Martínez and C. Cruz-Mendoza, A power optimization model for the long-term planning scenarios: Case study of Mexico's power system decarbonization, *The Canadian Journal of Chemical Engineering, 99*(4), 2020, 884–897.

[5] F. Mei, J. Zhang, J. Lu, Y. Jiang, Y. Gu, K. Yu, and L. Gan, Stochastic optimal operation model for a distributed integrated energy system based on multiple-scenario simulations, *Energy, 219*(2), 2020, 119629.1–119629.13.

[6] I. Mitiche, A. Nesbitt, S. Conner, P. Boreham, and G. Morison, 1D-CNN based real-time fault detection system for power asset diagnostics, *IET Generation Transmission & Distribution, 14*(24), 2020, 5766–5773.

[7] S. Chandrasekharan, S.K. Subramaniam, and B. Natarajan, Current indicator based fault detection algorithm for identification of faulty string in solar PV system, *IET Renewable Power Generation, 15*(7), 2021, 1596–1611.

[8] J. Shi, B. Foggo, and N. Yu, Power system event identification based on deep neural network with information loading, *IEEE Transactions on Power Systems*, *36*(6), 2021, 5622–5632.

[9] J. Hou, G. Song, P. Chang, R. Xu, and K.S.T. Hussain, Fault identification scheme for hybrid multi-terminal HVDC system based on control and protection coordination strategy, *International Journal of Electrical Power & Energy Systems, 136*, 2022, 107591.1–107591.13.

[10] C. Liang, H. Huan, T. Panyu, Y. Dong, Y. Haonan, and G. Noradin, Optimal modeling of combined cooling, heating, and power systems using developed African vulture optimization: a case study in watersport complex, *Energy Sources, Part A: Recovery, Utilization, and Environmental Effects, 44*(2), 2022, 4296–4317.

[11] P. Verrax, A. Bertinato, M. Kieffer, and B. Raison, Transient-based fault identification algorithm using parametric models for meshed HVDC grids, *Electric Power Systems Research, 185*, 2020, 106387.1–106387.16

[12] B. Gao, C. Peng, D. Kong, X. Wang, C. Li, M. Gao, and G. Noradin, Optimum structure of a combined wind/photovoltaic/fuel cell-based on amended Dragon fly optimization algorithm: A case study, *Energy Sources, Part A: Recovery, Utilization, and Environmental Effects, 44*(3), 2022, 7109–7131.

[13] W. Cai, R. Mohammaditab, G. Fathi, K. Wakil, A.G. Ebadi, and N. Ghadimi, Optimal bidding and offering strategies of compressed air energy storage: A hybrid robust-stochastic approach, *Renewable Energy, 143*, 2019, 1–8.

[14] S. Zuloaga and V. Vittal, Integrated electric power/water distribution system modeling and control under extreme mega drought scenarios, *IEEE Transactions on Power Systems, PP*(99), 2020, 474–484.

[15] B. Sharan and T. Jain, Spectral analysis-based fault diagnosis algorithm for 3-phase passive rectifiers in renewable energy systems, *IET Power Electronics, 13*(16), 2020, 3818–3829.

[16] W. Liu, Simulation study on identification technology of transmission line potential hazards based on corona discharge characteristics, *International Journal of Computer Applications in Technology,* (4), 2021, 351–357.

[17] Q. Zhang, W. Ma, G. Li, J. Ding, and M. Xie, Fault diagnosis of power grid based on variational mode decomposition and convolutional neural network, *Electric Power Systems Research, 208*, 2022, 107871.1–107871.9.

[18] X. Wang, L. Zhang, and W.P. Heath, Wind turbine blades fault detection using system identification-based transmissibility analysis, *Insight: Non-Destructive Testing and Condition Monitoring, 64*(3), 2022, 164–169.

[19] A. Anand and S. Affijulla, Hilbert-Huang transform based fault identification and classification technique for AC power transmission line protection, *International Transactions on Electrical Energy Systems, 30*(10), 2020, e12558.1–e12558.15.

[20] L. Qi, L. Qiu, and X. Zhou, Fault diagnosis method of mechanical power system based on image processing technology, *International Journal of Advanced Robotic Systems, 17*(2), 2020, 1729881420914093.1–1729881420914093.13.

[21] Y.M. John, A. Sanusi, I. Yusuf, and U.M. Modibbo, Reliability analysis of multi-hardware-software system with failure interaction, *Journal of Computational and Cognitive Engineering, 2*(1), 2023, 38–46.

[22] X. Deng, W. Wang, Y. Liao, Q. Zhang, S. Liu, and C. Wang, Study on online dispatching defensive strategy for power grid considering expected circuit breaker fault set, *Electric Power Systems Research, 203*, 2022, 107640.1–107640.13.

[23] E.N.V.D.V. Prasad and P.K. Dash, Fault analysis in photovoltaic generation based DC microgrid using multifractal detrended fluctuation analysis, *International Transactions on Electrical Energy Systems, 31*(3), 2020, 12564.1–e12564.20.

Biographies

Wenhua Guo is from Taiyuan City, Shanxi Province. She received the bachelor's degree from the School of Engineering, Shanxi University in June 2012 and the master's degree from Shanxi University in June 2016. Her research direction is smart grid. Since December 2016, she has been working as a Teacher with Shanxi Railway Vocational and Technical College. Her academic achievements are *Journal of Power Supply* "Control Method for Grid Formation in Offshore Wind Farms for DR-HVDC System Connection" was published on 22, 2024 (01); "Application of Photovoltaic Greenhouse Planting Technology" was published in the 2022 (09) issue of the "Use and Maintenance of Agricultural Machinery" (Provincial Journal); "Power Equipment Management" (National Journal) published in December 2022 titled "Application of Power Electronics Technology in Smart Grid."